Rap1 GTPase Regulation of Adherens Junction Positioning and Cell Adhesion

Andrea L. Knox* and Nicholas H. Brown†

Cell-cell junctions are distributed evenly around the lateral circumference of cells within an epithelium. We find that the even distribution of adherens junctions is an active process that requires the small guanosine triphosphatase Rap1. Cells mutant for *Rap1* condensed their adherens junctions to one side of the cell. This disrupted normal epithelial cell behavior, and mutant cell clones dispersed into the surrounding wild-type tissue. Rap1 is enriched at adherens junctions, particularly between newly divided sister cells where it may reseal the adherens junction ring. The regulation of adherens junction positioning could play a role in cell mobility and cell division.

Cells within an epithelium are linked by several types of junctions. Encircling the apical ends of cells are adherens junctions, which link to the actin cytoskeleton intracellularly and can thereby transmit force across the lateral plane of the epithelium (*1*). Although much attention has been paid to the regulation of apico-basal localization of adherens junctions (*2*), little is known about the mechanisms that underlie their even distribution around the cell circumference. Rap1 is a small guanosine triphosphatase (GTPase) of the Ras family (*3*) that has a role in regulating *Drosophila* morphogenesis (*4*) through an undetermined mechanism. During *Drosophila* wing development, epithelial cells related by lineage normally stay in a coherent group (*5*). However, clones of cells mutant for *Rap1* (*6*) dispersed into surrounding wild-type tissue (Fig. 1), indicating that loss of Rap1 function disrupts the normal cell-cell adhesion mechanism that keeps lineage-related cells in a coherent group. This phenotype has not been observed for other mutations studied by clonal analysis, including loss-of-function mutations in related GTPases such as Rho1 and Ras85D (*7*, *8*). Cells lacking Rap1 function still respect the lineage restriction at the anterior-posterior compartment boundary [Web fig. 1 (*9*)]. Observations of shape defects in *Rap1* mutant cells suggested that Rap1 might regulate apical cell-cell adhesion. Pupal wing cells mutant for *Rap1* lacked the normal hexagonal shape, and the area of the apical, but not the basal, surface was reduced relative to that of wild-type cells [Fig. 1C (*10*)]. Dispersed mutant cells were often observed in pairs or groups of four cells [43 and 23%, respectively (*11*)].

To assess the role of Rap1 in cell-cell adhesion, we examined the subcellular localization of adherens junctions and the adjacent, more basal, septate junctions. In contrast to their even distribution around the apical circumference of wild-type epithelial cells, adherens junction components—including the cell-surface adhesion protein DE-cadherin (Fig. 2, A and D) and two cytoskeletal proteins, α-catenin [visualized with a green fluorescent protein (GFP)–α-catenin fusion protein (Fig. 3, A and B)] and β-catenin (*10*)—were found predominantly on one side of *Rap1* mutant pupal wing cells. In a count of 856 cells containing such clusters of adherens junction components, 702 cells (82%) had adherens junctions condensed into a contact with just one neighboring cell. Clusters were also seen between a mutant cell and 2 other mutant cells (121 cells, 14%), or connecting a mutant cell with 3, 4, or 5 neighboring mutant cells (33 cells, 4%). Clusters of adherens junction proteins were observed only at interfaces between mutant cells, and not between a mutant and a wild-type cell. At interfaces between mutant and wild-type cells, normal levels of adherens junctions were observed.

Two proteins that may form a molecular link between Rap1 and adherens junctions are the multidomain cytoskeletal linker proteins AF6/canoe and ZO-1. Both AF6 and its *Drosophila* ortholog canoe bind to activated Rap1 (*12*, *13*), and canoe interacts with ZO-1 (*14*). Vertebrate ZO-1 binds to the adherens junction component α-catenin (*15*), thus completing a possible link from Rap1 to adherens junctions. Both canoe and ZO-1 localize to adherens junctions in normal *Drosophila* epithelia (*14*, *16*) and like the other adherens junction components, they distributed primarily to one side of *Rap1* mutant cells (Fig. 2, B and E). Although ZO-1 also participates in vertebrate tight junctions (*17*) and may be present in *Drosophila* septate junctions (*14*), there was not a comparable alteration in septate junction–associated proteins in *Rap1* mutant cells. The MAGUK protein Discs large (Fig. 2C) and the band 4.1 ortholog coracle (*10*) were evenly distributed around the circumference of *Rap1* mutant cells. Thus, loss of Rap1 function specifically impairs even distribution of adherens junctions around the cell circumference. The maintenance of septate junctions could explain how *Rap1* mutant cells still retain enough cell adhesion to remain within the epithelium.

The misplacement of adherens junctions in *Rap1* mutant clones suggests that dispersion

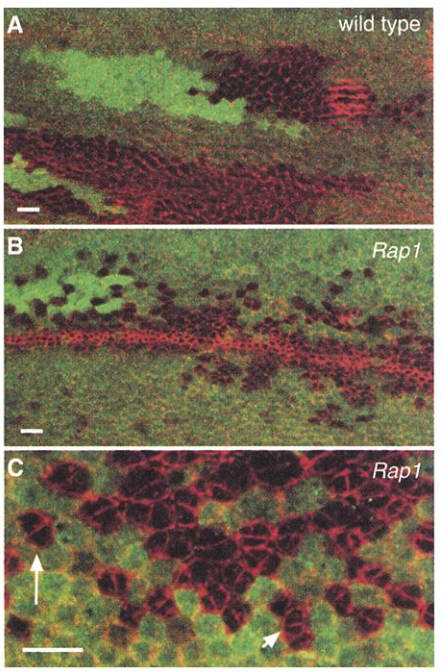

Fig. 1. Clones of wing cells mutant for *Rap1* lose their normal cohesion. Mitotic recombination was induced in flies heterozygous for a nuclear green fluorescent protein marker (*+/nls-GFP*). The small number of cells that have undergone recombination divided to produce a cell lacking GFP (+/+) and a sister cell with two copies of nls-GFP (*nls-GFP/nls-GFP*) (*6*). Six days later the progeny of each cell were observed in the developing wings of the pupa as groups of cells (clones), either lacking GFP or containing a double dosage (GFP staining is in green, and Phalloidin staining of actin is in red). In wild-type animals (**A**), both clones have discrete borders; two recombination events have occurred in this wing, producing two pairs of clones. (**B**) Clones produced in a *Rap1* heterozygote (*Rap1/nls-GFP*) resulted in Rap1 mutant clones lacking GFP, which have intermingled with surrounding wild-type cells (either *Rap1/nls-GFP* or *nls-GFP/nls-GFP*). (**C**) Higher magnification of *Rap1* mutant clones reveals that mutant cells had aberrant shapes and dispersed into wild-type tissue commonly in pairs (arrow) or fours (arrowhead). Bars, 10 μm.

Wellcome/CRC Institute and Department of Anatomy, University of Cambridge, Cambridge CB2 1QR, UK.

*Present address: Royal Society of New Zealand, 4 Hallswell Street, Wellington, New Zealand.

†To whom correspondence should be addressed at Wellcome/CRC Institute, Tennis Court Road, Cambridge CB2 1QR, UK. E-mail: nb117@mole.bio.cam.ac.uk

could be due to sorting caused by differential adhesion. L fibroblasts transfected with P-cadherin sort according to their level of cadherin expression (*18*), and such differential adhesion plays a role in *Drosophila* oocyte positioning at the posterior of the egg chamber (*19*, *20*). The *Rap1* mutant cell-dispersal phenotype may be an additional in vivo example of cell sorting according to differential DE-cadherin–mediated adhesion, although in this case, the amount of adhesion is altered by the failure to distribute adherens junctions evenly around the cell circumference, rather than by altered overall cadherin expression. Provided that the quantity of adherens junction components reflects the strength of adhesion, *Rap1* mutant cells could have adhered most strongly to mutant cells on the sides of the cell containing adherens junction clusters, very weakly to other mutant cells, and at normal strength to adjacent wild-type cells. Adhesion between mutant and wild-type cells that was stronger than adhesion between most *Rap1* mutant cells could have drawn small groups of mutant cells into wild-type tissue (Web fig. 2). These results suggest that regulation of the subcellular distribution of cell-cell junctions could play a role in the mobility and invasiveness of cells within an epithelium.

Because adherens junctions are also misplaced in undispersed *Rap1* mutant cells, misplacement is likely to be the cause rather than the consequence of cell dispersal. In this case, mislocalization of adherens junctions during wing development should precede cell dispersal. Clonal cells mutant for *Rap1* in the late (wandering) third-instar imaginal disc

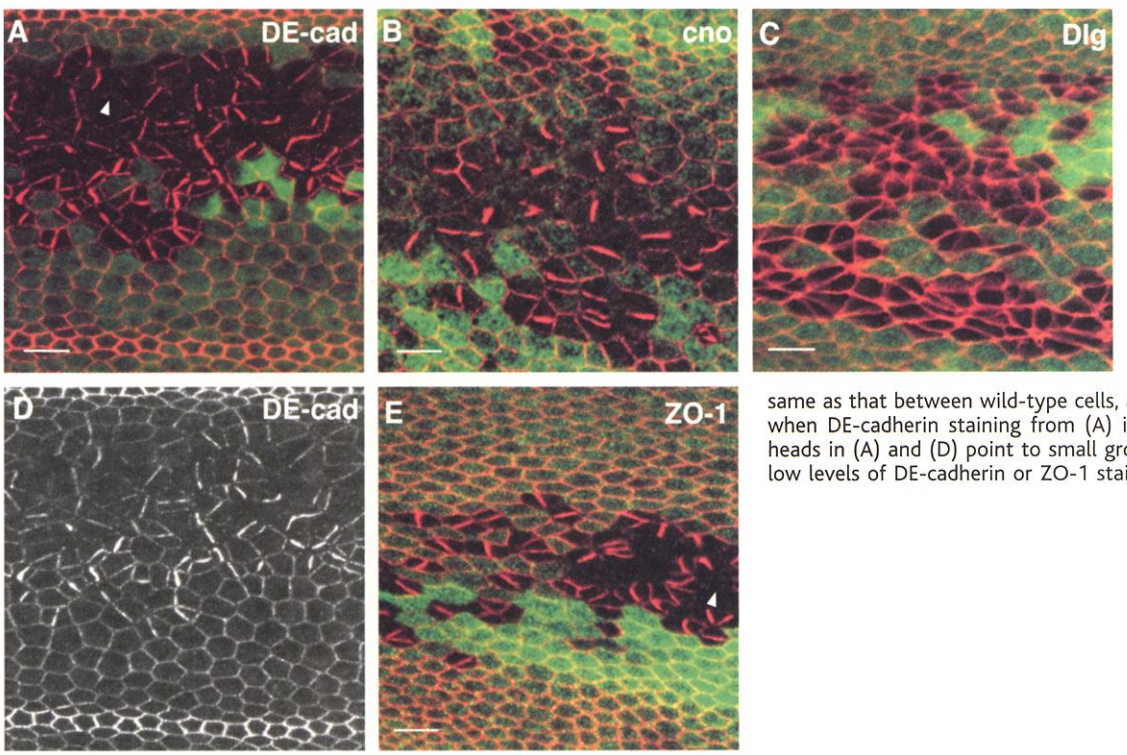

Fig. 2. The even distribution of adherens junctions is disrupted in *Rap1* mutant clones, but septate junction positioning is not altered. Pupal wings containing *Rap1* mutant clones marked by the absence of GFP (green) were stained (red) for DE-cadherin (**A**), canoe (**B**), ZO-1 (**E**), and Discs large (**C**) (*6*). The level of adherens junction proteins at the interface between *Rap1* mutant and wild-type cells was the same as that between wild-type cells, as can be seen more clearly when DE-cadherin staining from (A) is shown alone (**D**). Arrowheads in (A) and (D) point to small groups of cells that have very low levels of DE-cadherin or ZO-1 staining. Bars, 10 μm.

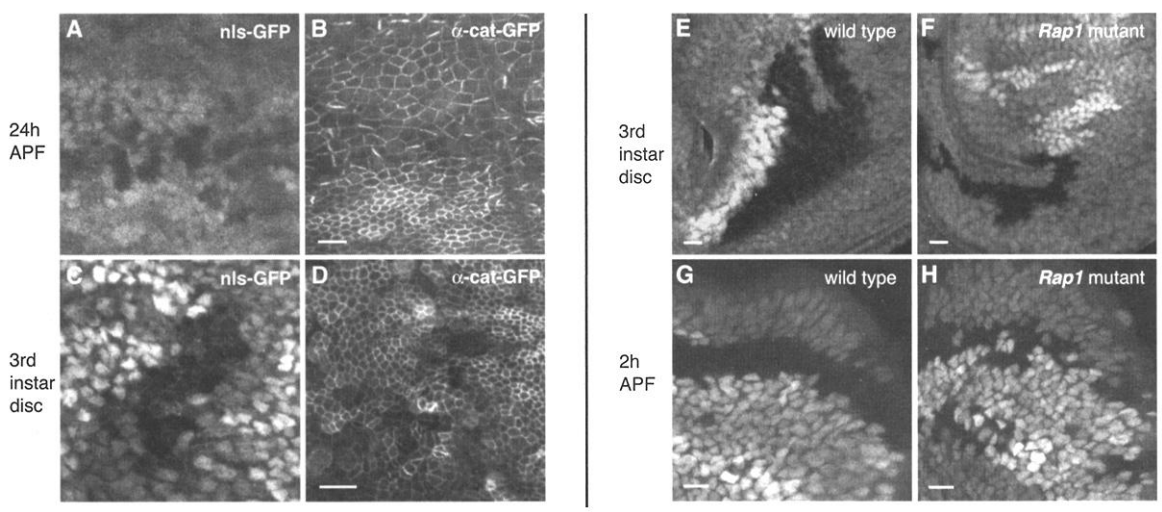

Fig. 3. The aberrant adherens junction distribution caused by loss of Rap1 is seen in the imaginal disc, but mutant cell dispersal does not begin until wing disc evagination. (**A**, **C**, **F**, **H**) Clones of *Rap1* mutant cells are distinguished by the absence of nuclear nls-GFP (*22*). (**B** and **D**) The adherens junctions are visualized with α-catenin–GFP, which showed the same aberrant distribution in 24-hour APF pupal wings (A and B) as seen with the other adherens junction markers in Fig. 2. Altered α-catenin–GFP distribution is also seen in *Rap1* mutant clones in the larval imaginal disc (C and D). As compared with wild-type clones (**E**), *Rap1* mutant imaginal disc clones do not disperse (F). However, 2 to 3 hours later during wing disc evagination, dispersal of *Rap1* mutant clones is seen (H) [compare with the wild-type clone in (**G**)]. Bars, 10 μm.

did not disperse (Fig. 3, E and F), yet the adherens junction component α-catenin was already mislocalized (Fig. 3, C and D), indicating that adherens junction mislocalization precedes dispersal. The larvae pupariate within a few hours of this time, and dispersal of *Rap1* mutant cells was first observed 2 hours after pupariation (Fig. 3, G and H). Evagination of the disc during this time period requires extracellular protease activity, which is thought to loosen cell-cell and cell-extracellular matrix contacts, allowing cell rearrangements and shape changes to occur (*21*). Cell rearrangements can be observed as the elongation of marked clones; therefore, cells normally exchange neighbors even if they do not normally mix. Loosening of extracellular contacts likely allows *Rap1* mutant cells to mix with their wild-type neighbors. Consistent with this, cell dispersion was initially more pronounced at the distal end of the evaginating wing (*10*), where cell rearrangements are first initiated (*21*).

To investigate whether Rap1 recruitment to adherens junctions is involved in aberrant junction distribution in mutant cells, we expressed a transgene encoding a GFP-Rap1 fusion protein. This fusion protein is under the control of the endogenous *Rap1* promoter and was expressed ubiquitously throughout development (*22*, *23*). In normal wing imaginal disc cells, GFP-Rap1 was broadly distributed in the cytoplasm and basolateral membrane and highly concentrated at the position of the adherens junctions (Fig. 4C), consistent with the possible interaction of Rap1 with adherens junction proteins canoe and ZO-1. Despite its own polarized distribution, Rap1 was not required for normal apico-basal distribution of adherens junctions; α-catenin was located apically in *Rap1* mutant imaginal disc clones (Fig. 4D). β-Catenin and DE-cadherin also did not mislocalize along the apico-basal axis in *Rap1* mutant pupal wing clones (*10*).

The distribution of GFP-Rap1 in dividing cells suggests a mechanism by which Rap1 might normally act to ensure even adherens junction distribution. Dividing cells in the wing imaginal disc retain their adherens junctions with surrounding cells (*24*), and the localization of GFP-Rap1 was not altered during division (Fig. 5A). However, GFP-Rap1 was consistently enriched at the junction between newly formed sister cells (Fig. 5B). A transient enrichment of GFP-Rap1 between sister cells in the epidermis of living embryos was also observed (Web fig. 3). Hence, Rap1 may reorganize the adherens junction ring subsequent to or during late cytokinesis to ensure that appropriate amounts of adherens junctions are maintained around the circumference of new cells.

One model explaining how loss of Rap1 function during cytokinesis leads to adherens junction clustering is as follows. Maintenance of adherens junction distribution throughout cell division requires a mechanism to convert the single adherens junction ring into two rings, involving breaking and resealing of the ring during cytokinesis. Rap1 could be essential for this process. Failure to reseal the adherens junction ring could allow it to recoil to one side of the cell (Web fig. 4), driven by contraction of the actin and myosin present in the ring (*21*). This would cause rearrangement of cadherin contacts into clusters on sides adjacent to mutant cells with a similar defect, but not on the sides of the cell contacting wild-type cells, where cadherin distribution is stabilized at a normal density. Clusters would most likely form at the interface between sister cells, because both cells' rings recoil at the same time. However, clusters could also form between two adjacent mutant cells that are not sisters if they were in a similar state at the same time. Accordingly, the 14% of clusters between one mutant cell and two others demonstrates that clusters were present at interfaces between cells that are not sisters from their most recent division. Further rounds of division could lead to segregation of clusters into just one daughter cell, producing cells with few adherens junctions, as seen within some *Rap1* mutant clones (Fig. 2, A and E).

Rap1 maintains circumferential adherens junction distribution in cells and thus shares with Rho GTPase family members the ability to regulate the cytoskeleton and cell adhesion. Thus, its demonstrated role in morphogenetic processes that are driven by adhesion-dependent cell shape changes and movements (*4*) may involve regulation of the link between the cytoskeleton and adherens junctions.

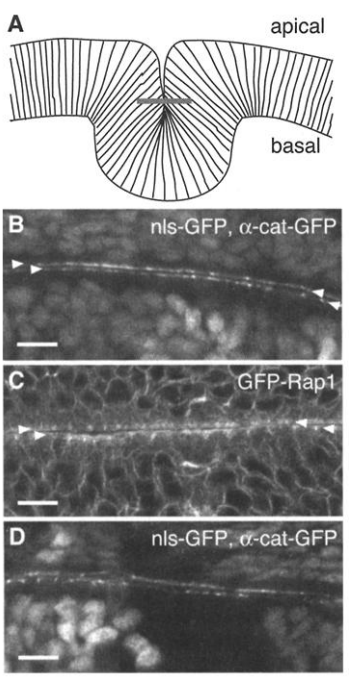

Fig. 4. GFP-Rap1 is enriched at the site of adherens junctions, but is not required for apico-basal adherens junction positioning (*22*). (**A**) Diagram of the plane of focus for (B), (C), and (D). The gray bar represents the position at which sections were taken across a characteristic fold in third-instar wing imaginal discs. Apical cell edges face the inside of the fold. (**B**) Disc expressing nls-GFP and α-catenin–GFP, showing the two apical rows of adherens junctions (arrowheads). (**C**) Disc expressing GFP-Rap1. GFP-Rap1 is in the cytoplasm, associated with the basolateral membrane, and enriched at the position of adherens junctions (arrowheads). (**D**) α-Catenin–GFP in a *Rap1* clone marked by the absence of nls-GFP. Apico-basal positioning of α-catenin–GFP is not altered in *Rap1* cells. Bars, 10 μm.

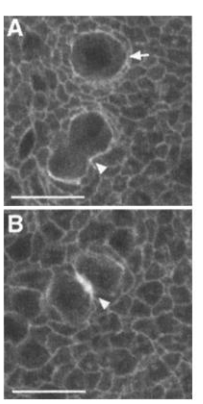

Fig. 5. GFP-Rap1 is enriched at the junction between newly divided sister cells (*22*). (**A**) In the third-instar wing imaginal disc, cortical GFP-Rap1 is distributed evenly in cells in metaphase (arrow) and early cytokinesis (arrowhead). (**B**) GFP-Rap1 is enriched at the junction between sister cell pairs (arrowhead). Bars, 10 μm.

References and Notes

1. A. Kusumi, K. Suzuki, K. Koyasako, *Curr. Opin. Cell Biol.* **11**, 582 (1999).
2. H. A. Muller, *Dev. Dyn.* **218**, 52 (2000).
3. G. M. Bokoch, *Biochem. J.* **289**, 17 (1993).
4. H. Asha, N. D. deRuiter, M. G. Wang, I. K. Hariharan, *EMBO J.* **18**, 605 (1999).
5. A. Garcia-Bellido, P. Ripoll, G. Morata, *Nature* **245**, 251 (1973).
6. Wild-type clones were generated by heat shocking *y w P{ry$^{+t7.2}$ hsFLP}22; P{w^{hs} FRT}2A/P{w^{+}nls-GFP} P{w^{hs} FRT}2A* flies and *Rap1* clones by heat shocking *y w P{ry$^{+t7.2}$ hsFLP}22; Rap1$^{P[5709]}$ P{w^{hs} FRT}2A/ P{w^{+}nls-GFP} P{w^{hs} FRT}2A* or *y w P{ry$^{+t7.2}$ hsFLP}22; Rap1^{B1} P{w^{hs} FRT}2A/ P{w^{+}nls-GFP} P{w^{hs} FRT}2A* flies (*25*, *26*). Identical results were obtained with two amorphic alleles of *Rap1*, *Rap1^{B1}* (*4*) and a P-element inserted into the coding region, *Rap1$^{P[5709]}$*(*23*). For actin staining of pupal wings 30 to 36 hours after puparium formation (APF) (*27*), we used rhodamine-conjugated phalloidin (Molecular Probes). For antibody stains (*27*), we used DCAD2 anti–DE-cadherin (*28*), anti-cno (*14*), anti-ZO-1 (*29*), and anti-Dlg (*30*). All wings were fixed and stained at 30 to 36 hours APF, except for wings stained for canoe, which were aged 24 hours APF. Images were visualized with a MRC1024 confocal microscope (Bio-Rad).
7. F. J. Diaz-Benjumea, E. Hafen, *Development* **120**, 569 (1994).
8. D. I. Strutt, U. Weber, M. Mlodzik, *Nature* **387**, 292 (1997).
9. Supplemental data are available on *Science* Online at www.sciencemag.org/cgi/content/full/295/5558/1285/DC1.
10. A. L. Knox, N.H. Brown, unpublished observations.
11. The size of groups of dispersed *Rap1* mutant cells was counted in 23 clones from 21 different wings aged between 24 and 36 hours APF. The number of dispersed groups of a given size (and fraction of the total 244 groups) was as follows: 13 (5%) single cells; 106 (43%) cell pairs; 20 (8%) 3-cell groups; 56 (23%) 4-cell groups; 8 (3%) 5-cell groups; 16 (7%) 6-cell groups; and 25 (10%) groups of 7 or more cells.
12. T. Linnemann *et al.*, *J. Biol. Chem.* **274**, 13556 (1999).

13. B. Boettner, L. VanAelst, U. Gaul, personal communication
14. K. Takahashi, T. Matsuo, T. Katsube, R. Ueda, D. Yamamoto, *Mech. Dev.* **78**, 97 (1998).
15. M. Itoh, A. Nagafuchi, S. Moroi, S. Tsukita, *J. Cell Biol.* **138**, 181 (1997).
16. X. Wei, H. M. Ellis, *Mech. Dev.* **100**, 217 (2001).
17. B. R. Stevenson, J. D. Siliciano, M. S. Mooseker, D. A. Goodenough, *J. Cell Biol.* **103**, 755 (1986).
18. M. S. Steinberg, M. Takeichi, *Proc. Natl. Acad. Sci. U.S.A.* **91**, 206 (1994).
19. D. Godt, U. Tepass, *Nature* **395**, 387 (1998).
20. A. Gonzalez-Reyes, D. St Johnston, *Development* **125**, 3635 (1998).
21. D. Fristrom, J. W. Fristrom, in *The Development of* Drosophila melanogaster, M. Bate, A. Martinez Arias, Eds. (Cold Spring Harbor Laboratory Press, Cold Spring Harbor, NY, 1993), vol. 2, pp. 843–896.
22. *Rap1* mutant wing clones expressing α-catenin–GFP (*31*) were generated by heat shocking *y w P{ry$^{+t7.2}$ hsFLP}22; P{UAS-DαC-GFP#3} {arm-GAL4}/+; Rap1$^{P[5709]}$ P{w^{hs} FRT}2A/ P{w^{+}nls-GFP} P{w^{hs} FRT}2A* flies. 24h APF pupae were dissected from the pupal case and directly mounted in Vectashield (Vector Labs, Burlingame, CA), then clones were imaged with a MRC1024 confocal microscope (Bio-Rad). Rap1 was tagged with GFP by generating a genomic rescue construct with GP inserted at the NH_2-terminus of Rap1 (*23*). Imaginal discs and 2-hour APF wings expressing GFP-Rap1 or α-catenin–GFP were fixed in 4% formaldehyde and mounted in Vectashield. Images were collected with a Radiance 2000 confocal microscope (Bio-Rad).
23. A. L. Knox, N. H. Brown, in preparation.
24. D. F. Woods, J. W. Wu, P. J. Bryant, *Dev. Genet.* **20**, 111 (1997).
25. T. B. Chou, N. Perrimon, *Genetics* **144**, 1673 (1996).
26. S. Luschnig, J. Krauss, K. Bohmann, I. Desjeux, C. Nusslein-Volhard, *Mol. Cell* **5**, 231 (2000).
27. D. Fristrom, M. Wilcox, J. Fristrom, *Development* **117**, 509 (1993).
28. H. Oda, T. Uemura, Y. Harada, Y. Iwai, M. Takeichi, *Dev. Biol.* **165**, 716 (1994).
29. M. Takahisa *et al.*, *Genes Dev.* **10**, 1783 (1996).
30. D. F. Woods, P. J. Bryant, *Cell* **66**, 451 (1991).
31. H. Oda, S. Tsukita, *Dev. Genes Evol.* **209**, 218 (1999).
32. We thank P. Bryant, R. Fehon, I. Hariharan, R. Howes, H. Oda, S. Luschnig, M. Takahisa, M. Takeichi, and D. Yamamoto for providing antibodies and fly stocks, and S. Bray, B. Harris, D. St Johnston, and R. White for critically reading the manuscript. We thank J. Overton for technical assistance and the members of our lab for valuable advice. Supported by a Wellcome Trust Senior Fellowship (N.H.B.) and grants from the Association of Commonwealth Universities, the New Zealand Federation of University Women, and Trinity College (A.L.K.).

29 October 2001; accepted 10 January 2002

Role of the Isthmus and FGFs in Resolving the Paradox of Neural Crest Plasticity and Prepatterning

Paul A. Trainor,* Linda Ariza-McNaughton,*† Robb Krumlauf‡

Cranial neural crest cells generate the distinctive bone and connective tissues in the vertebrate head. Classical models of craniofacial development argue that the neural crest is prepatterned or preprogrammed to make specific head structures before its migration from the neural tube. In contrast, recent studies in several vertebrates have provided evidence for plasticity in patterning neural crest populations. Using tissue transposition and molecular analyses in avian embryos, we reconcile these findings by demonstrating that classical manipulation experiments, which form the basis of the prepatterning model, involved transplantation of a local signaling center, the isthmic organizer. FGF8 signaling from the isthmus alters *Hoxa2* expression and consequently branchial arch patterning, demonstrating that neural crest cells are patterned by environmental signals.

The cranial neural crest is a pluripotent migratory cell population that plays a critical role in the construction of the vertebrate head, giving rise to the facial and visceral skeleton, most of the skull bones and connective tissue, and the neurons and glia of the peripheral nervous system (*1–3*). The highly conserved segmental organization of the vertebrate hindbrain into rhombomeres (*4*, *5*) plays a key role in patterning the identity and pathways of neural crest cell migration into the branchial arches (*6–12*). Currently, there is a fundamental paradox in mechanisms that pattern neural crest cells and their derivatives. Noden grafted first-arch neural crest precursors posteriorly to new locations in avian embryos, and these ectopic crest cells gave rise to duplications of first-arch skeletal derivatives, such as the quadrate and Meckel's cartilage. This landmark transposition study (*2*) led to the model that cranial neural crest cells are preprogrammed in the neural tube before their migration and that they passively carry positional information necessary for craniofacial morphogenesis from the neural tube to the periphery. This prepatterning model has shaped the way we think about craniofacial development during the past 18 years and has also been used to explain skeletal duplications observed in null mutations of A-P patterning genes, such as *Hoxa2* and *Hoxa3* (*13–15*). However, recent transposition and lineage tracing experiments contradict the prepatterning model, highlighting the plasticity of rhombomeres and cranial neural crest populations [(*11*, *12*, *16–23*) and reviewed in (*5*)]. These studies suggest an alternative dynamic model, in which neural crest patterning relies on a balance of instructive signals from the hindbrain, maintenance signals from the branchial arch environment, and cell community interactions.

In this study, we performed experiments aimed at understanding and resolving the basis for these conflicting models and results. An often-ignored aspect of Noden's analysis is that posterior transplantations of presumptive frontonasal or presumptive first-arch neural crest both produced the same quadrate and Meckel's cartilage duplications. Hence, the same ectopic structures formed irrespective of the axial origin of the neural crest cells. What links these different transplantations is the probable inclusion of the mid/hindbrain isthmus in the grafted tissue. In recent years, it has become apparent that local inductive centers, such as the mid/hindbrain junction (isthmus), play roles in anterior neural patterning (*24*). Noden used the isthmus as a morphological marker for delineating the neural tissue to be grafted posteriorly (Fig. 1A), and therefore one possible explanation for the conflicting results may relate to the inclusion of a localized signaling center along with neural crest progenitors.

To directly test this idea, we transplanted the isthmus posteriorly in place of rhombomere 4 (r4) in ovo, in stage-matched chick embryos at somite stage 8 to 9 (8-9) (Fig. 1, A through C). The donor isthmus included the mid/hindbrain junction and a small population of cells on both sides of the boundary (Fig. 1A). After 24 to 48 hours of in ovo culture, grafted embryos were assayed for effects on *Hoxa2* expression (Fig. 1, D and E), which is the primary determinant of the second branchial arch neural crest phenotype (*13*, *14*). *Hoxa2* expression in the second branchial arch neural crest was inhibited (Fig. 1E), and this was not due to an absence of migrating neural crest cells, because 1,1'-dioctadecyl-3,3,3',3'-tetramethylindocarbonocyanine perchlorate (DiI) labeling of the transplanted tissue shows that numerous

The Stowers Institute for Medical Research, 1000 East 50th Street, Kansas City, MO 64110, USA, and Division of Developmental Neurobiology, The National Institute for Medical Research, London, UK, NW7 1AX.

*These authors contributed equally to this paper.
†Present address: The Sanger Centre, Wellcome Trust Genome Campus, Hinxton, Cambs CB10 1SA, UK.
‡To whom correspondence should be addressed at The Stowers Institute for Medical Research, 1000 East 50th Street, Kansas City, MO 64110, USA. E-mail: rek@stowers-institute.org